Vol. 20, No. 2 (2021) 581-605
Revista Mexicana de Ingeniería Química

K_2HPO_4- pretreatment significantly enhances the biosorption capacity of Co^{2+} by *Lemna gibba*

El pretratamiento con K_2HPO_4 mejora significativamente la capacidad de biosorción de Co^{2+} de *Lemna gibba*

J.L. Reyes-Ledezma, A.E. Ramírez-Rodríguez, C.B. Ballinas-Cesatti, E. Cristiani-Urbina, L. Morales-Barrera*

Departamento de Ingeniería Bioquímica. Escuela Nacional de Ciencias Biológicas. Instituto Politécnico Nacional. Av. Wilfrido Massieu s/n, Unidad Profesional Adolfo López Mateos, 07738, Mexico City, Mexico

Received: September 19, 2020; Accepted: January 5, 2021

Abstract

Since divalent cobalt [Co^{2+}] in wastewater is highly toxic, it must be removed before dumping the water into the environment. The aim of this study was to examine the biosorption of Co^{2+} by *Lemna gibba* (LG) after pretreatment with various compounds to improve its biosorption capacity. The pretreatment with K_2HPO_4 (0.1 M) produced the best biosorption capacity of Co^{2+} by LG (31.21 ± 0.29 mg g^{-1} vs 18.87 ± 0.19 mg g^{-1} for the untreated control). Subsequently, the optimal concentration (0.3 M) of K_2HPO_4 was found (the pretreatment herein denominated PLG), showing a biosorption capacity of 40.13 ± 0.18 mg g^{-1} at pH 7.0. The pseudo-second order model most adequately fit the experimental kinetics. According to the proximate chemical analysis, the pretreatment enhanced the biosorption capacity (PLG vs LG), probably by improving sorption site availability through the elimination of salts, and by increasing the negative charge of the plant cell surface (from -26 to -35 mV), thus favoring the approach of positively charged Co^{2+}. The ATR-FTIR analysis of PLG demonstrated that its hydroxyl, carboxyl, amide and amine groups importantly contributed to Co^{2+} removal. Thus, PLG is a promising biosorbent material for Co^{2+} removal from aqueous solutions.

Keywords: Divalent cobalt, *Lemna gibba*, biosorption, pretreatment, zeta potential, ATR-FTIR.

Resumen

Debido a la toxicidad del cobalto divalente [Co^{2+}], éste debe eliminarse de las aguas residuales antes de verterlas al ambiente. El objetivo de este estudio fue examinar la capacidad de biosorción de Co^{2+} por *Lemna gibba* (LG) después de pretratarla buscando mejorar dicha capacidad. El pretratamiento con K_2HPO_4 (0.1 M) produjo la mayor biosorción de Co^{2+} (31.21 ± 0.29 mg g^{-1} vs 18.87 ± 0.19 mg g^{-1} de LG sin tratar). Posteriormente, se encontró que la concentración óptima de K_2HPO_4 fue de 0.3 M (este biosorbente se denominó PLG), mostrando una capacidad de biosorción de 40.13 ± 0.18 mg g^{-1} a pH 7.0. El modelo de pseudo-segundo orden se ajustó adecuadamente a la cinética experimental. Según el análisis químico proximal, el pretratamiento mejoró la biosorción (PLG vs LG), probablemente al aumentar la disponibilidad de los sitios de sorción mediante la eliminación de sales y al incrementar la carga negativa de la superficie de la planta (de -26 a -35 mV), favoreciendo así el acercamiento del Co^{2+}. El análisis ATR-FTIR de PLG demostró que sus grupos hidroxilo, carboxilo, amida y amina contribuyen a la remoción de Co^{2+}. Por tanto, PLG es un biosorbente prometedor para la eliminación de Co^{2+} de soluciones acuosas.

Palabras clave: Cobalto divalente, *Lemna gibba*, biosorción, pretratamiento, potencial zeta, ATR-FTIR.

1 Introduction

Cobalt is a heavy metal found in natural form in minerals of the Earth's crust, most commonly associated with sulfur, iron, copper and nickel (Cheang and Mohamed, 2016). In trace quantities, cobalt is an essential nutrient for certain physiological functions of human beings, principally as a constituent of vitamin B12 (Shahat *et al*., 2015; Vilvanathan and Shanthakumar, 2015; Anirudhan *et al*., 2016). However, at concentrations beyond such trace amounts, this heavy metal is very toxic for humans.

* *Corresponding author. E-mail*: lmoralesb@ipn.mx
https://doi.org/10.24275/rmiq/IA2042
ISSN:1665-2738, *issn-e*: 2395-8472

Cobalt is a raw material for the petrochemical, mining, metallurgy and electroplating industries, and for the manufacture of electronics, alloys, food coloring, pigments and lithium batteries as well as the tanning of hides (Abbas *et al*., 2014; Shahat *et al*., 2015; Anirudhan *et al*., 2016; Leyssens *et al*., 2017). Due to its many uses, cobalt is frequently part of industrial wastewater. The accumulation of cobalt in ecosystems (microorganisms, aquatic flora and aquatic fauna) can persist in the food chain and lead to environmental damage and human health problems (Abbas *et al*., 2014). Exposure to cobalt can cause minor problems (e.g., dermatitis, depression and fatigue) as well as more serious illnesses (e.g., liver, gastric, neurological, cardiovascular and endocrine disorders; asthma, irritation of the respiratory tract and pneumonia) (He *et al*., 2011; Cheang and Mohamed, 2016; Leyssens *et al*., 2017). Therefore, it is necessary to treat affected wastewater before discharging it into the sewer system or a body of water.

Heavy metals are removed from water with many conventional methods, including chemical precipitation, ion exchange, oxidation/reduction, filtration, electrochemical treatment, reverse osmosis and membrane technology (Ahluwalia and Goyal, 2007; Mamba *et al*., 2009). Whereas some of these methods are not very efficient for the removal of low concentrations of metals, others are efficient but costly in terms of economic and energy requirements (Vullo *et al*., 2008). Consequently, biotechnological processes for the removal of heavy metals that are both efficient and economical, such as biosorption, have been given great stimulus (Mamba *et al*., 2009; Moradi *et al*., 2020).

Biosorption is an innovative technique known for its economical and efficient removal of pollutants from water (García-González *et al*., 2016). Among the active and inactive biological materials employed for this purpose are plants, algae, bacteria, fungi, and even industrial waste or by-products (Abd El Hameed *et al*., 2015; Moreno-Rivas *et al*., 2016; Villabona-Ortíz *et al*., 2019; Fawzy *et al*., 2020). Biosorbents bear polysaccharides, lipids and proteins on their surface, conferring them with diverse functional groups (e.g., carbonyl, sulfhydryl, amine, sulfate, phenol, carboxyl, amide and hydroxyl groups) capable of the uptake of contaminants. These functional groups are able to remove heavy metals, food coloring, phosphates, pharmaceuticals and hormones from aqueous solutions (Volesky, 2003; Huang *et al*., 2008; Huang *et al*., 2014; Daughton, 2014; Ramírez-Rodríguez *et al*., 2018; Reyes-Ledezma *et al*., 2020). The properties of biomaterials can be modified by some physical and chemical pretreatments to enhance their biosorption capacity (Adeniyi and Ighalo, 2019; Zafar *et al*., 2019).

In the present study, the aquatic plant *Lemna gibba* (LG) (swollen duckweed) was used as a biosorbent. This macrophyte is commonly disseminated in grand extensions of canals, ponds and lakes, which not only makes navigation difficult but also impedes the passage of light beyond the surface of the water and thus diminishes photosynthesis and the production of oxygen necessary for a healthy aquatic environment. Consequently, LG is considered a plague (Zetina *et al*., 2010), but has characteristics that make it a promising material for the removal of heavy metals and other contaminants from bodies of water (Khataee *et al*., 2012).

The aim of the current contribution was to test the capacity of LG as a biosorbent of divalent cobalt (Co^{2+}) from an aqueous solution. The biosorbent capacity was increased by different chemical pretreatments and the best one was chosen for further analysis. The characteristics of the untreated and pretreated biosorbent were compared to elucidate the specific modifications in the biomaterial that allowed for the improvement of its biosorption capacity. The functional groups in *Lemna gibba* (untreated and pretreated) responsible for the removal of Co^{2+} from the aqueous solution were identified with Fourier-transform infrared spectroscopy by attenuated total reflection (ATR-FTIR).

2 Materials and methods

2.1 Chemicals

The chemicals employed were of analytical grade, purchased from JT Baker® (>90% purity). A standard solution was prepared of 1 g of Co^{2+} L^{-1} from a hexahydrate of cobalt chloride salt ($CoCl_2 \cdot 6H_2O$, JT Baker®, >98% purity) mixed with type II deionized water. The initial and residual concentration of cobalt in the assays was determined by the dimethylglyoxime (DMG) method.

2.2 Biomaterials

Lemna gibba (LG) was collected from the "Canal de Zacapa" (Zacapa Canal) in Mexico City, Mexico (19°15'31.8"N 99°05'05.3"W). The plant was first

washed with tap water until eliminating the dirt, slime and residues of insects and mollusks characteristic of canals. It was then washed again with type II water and dried in trays in a Luzeren™ oven at 60 ºC for 48 h. Once the plant was dry, it was ground in a Glen Creston™ hammer mill. Later, it was passed through standard ASTM sieves to obtain particles of a uniform size (300-500 μm). One part of the LG sample was used to examine its biosorption capacity. The rest was subdivided into groups to be submitted to different pretreatments. LG was pretreated by putting 5 g L^{-1} of the plant material in contact with distinct solutions under the following conditions of temperature and time (Reyes-Ledezma, 2017):

- Water for 30 min at two temperatures: room temperature (rt, being approximately 18 ºC) and 60 ºC.
- Neutral salts: NaCl and $MgSO_4$ (both at 0.1 M) at rt for 30 min.
- Organic solvents: 1% v/v acetone and 1% v/v hexane at rt for 30 min.
- Acids: HCl, H_2SO_4, CH_3COOH, NH_4Cl and HNO_3 (all at 0.1 M) at rt for 4 h.
- Alkalis: NaOH and KOH (both at 0.1 M) at rt for 15 min; Na_2CO_3, $NaHCO_3$, KH_2PO_4 and K_2HPO_4 (all at 0.1 M) at rt for 30 min.

During the pretreatment, the material was subjected to constant shaking at 140 rpm in an All Sheng™ orbital shaker. Subsequently, the biosorbent was washed with distilled water until the wash water reached a near neutral pH, and then the plant material was dried in a Luzeren™ oven at 60 ºC for 48 hours. Untreated LG and the 17 pretreated LG samples were conserved in bottles (hermetically closed and clearly labeled) at rt until further use.

2.3 Biosorption studies

2.3.1 Evaluation of the biosorption capacity of the biosorbents

An aqueous solution of cobalt (120 mL with an initial concentration of 100 mg L^{-1} and pH 7.0) was poured into 500 mL Erlenmeyer flasks. A sample was collected from each flask to determine the initial concentration of cobalt, and then 0.12 g of LG was placed in a flask and 0.12 g of the various pretreated LGs were placed in other flasks to attain a total concentration of 1 g L^{-1} of biosorbent. The suspensions were left for two hours under constant shaking at 140 rpm in an All Sheng™ orbital shaker at rt. At different times during this period, samples were taken and filtered through grade 42 Whatman™ paper to obtain a solution free of biosorbent. The filtered samples from each flask were utilized in the corresponding dilutions for the quantification of the residual concentration of cobalt. During the time of the assay, the pH of the suspensions in each flask was maintained constant at 7.0 by using HCl and NaOH (0.01 M and 0.1 M). DMG forms an amber complex with Co^{2+}, the intensity of which is directly proportional to the concentration of the ion in the solution. The absorbance of the samples was read on a spectrophotometer (Genesys 10 UV/VIS, Thermo Electron Scientific Instruments Corporation) at 400 nm (Gramlich *et al.*, 2011). Based on the predetermined initial concentrations and residues of cobalt, the biosorption capacity was calculated in the following manner (Eq. 1):

$$q_t = \frac{c_i - c_t}{X} \tag{1}$$

where q_t is the biosorption capacity (mg g^{-1}) at the time (t) the sample was taken, C_i and C_t represent the initial and residual concentration of Co^{2+} (mg L^{-1}) in the solution at time t_i = 0 h and $t = t$, respectively, and X is the concentration of the biosorbent employed (g L^{-1}). Once the system has reached equilibrium, the biosorption capacity corresponds to q_{eq} ($q_t = q_{eq}$) and the residual concentration of Co^{2+} is $C_t = C_{eq}$. With this data, kinetic modeling was carried out for the biosorption of Co^{2+} by LG and the 17 pretreated LG samples. Controls free of biosorbent were included to analyze the possible abiotic changes in the concentration of cobalt.

2.3.2 Selection of the pretreatment and its subsequent optimization

For the comparison of the biosorption of Co^{2+} by LG vs the pretreated LG samples, one parameter used was the behavior index (BI), which relates one condition or problem (the pretreatment) to the control (LG), as defined by Eq. 2 (Hernández-Estévez and Cristiani-Urbina, 2014):

$$BI = \frac{\left(\int_{t_i}^{t_f} g_t dt\right)_{problem} - \left(\int_{t_i}^{t_f} g_t dt\right)_{control}}{\left(\int_{t_i}^{t_f} g_t dt\right)_{control}} 100 \tag{2}$$

where the integral of $q_t dt$ is the area under the curve given by the model that best defined the kinetics of biosorption of Co^{2+} by the pretreated LG (problem) and the untreated biosorbent (LG, control) at t_i (0 h) and t_f (2 h, the total time of the assay). The integration was computed on Wolfram Mathematica ver. 9.0 software (Wolfram Research, Inc.). According to the equation, $BI > 0$ shows an increase in the capacity of LG for the biosorption of cobalt, $BI < 0$ denotes a decrease in the same, and $BI = 0$ indicates a null effect. Based on the results, the most appropriate pretreatment for the biosorption of Co^{2+} was chosen.

With the aim of examining the possibility of improving the capacity of removal of Co^{2+} by the pretreatment selected, the latter was evaluated at different concentrations in solution. The kinetics of biosorption was studied by following the previously described procedures. The capacity of the biosorption of cobalt and the *BI* were determined. Additionally, the kinetics of biosorption were modeled for the distinct concentrations of the chosen pretreatment. With these parameters, the concentration of the pretreatment showing the best capacity for the removal of Co^{2+} was defined. For practical purposes, this pretreatment is hereafter denominated PLG.

2.4 *Determination of the kinetic model of biosorption*

Several mathematical models (Eqs. 3-6) were utilized to model the experimental data obtained during the evaluation of the biosorption capacity in relation to time (Table 1).

2.5 *Statistical analysis*

All experiments involved at least two independent assays and the evaluation of each sample was performed in triplicate (n = 6). Differences between groups were examined by two-way analysis of variance (ANOVA) followed by Tukey's test for multiple comparisons on GraphPad Prism™ 8.4. Data are expressed as the mean ± standard deviation. The time required to reach equilibrium (t_{eq}) and the experimental biosorption capacity at equilibrium (q_{e-exp}) were established with the same statistical method. The parameters of the models were calculated by linear regression on GraphPad Prism™ 8.4. The kinetic model was selected by comparing R^2 (the correlation coefficient squared) and the error functions: sum of squares (SS), standard deviation of the residuals (Syx), and the corrected Akaike information criterion ($AICc$).

2.6 *Characterization of the biosorbent*

The untreated biosorbent (LG) and the plant material subjected to the best pretreatment (PLG) were characterized with the following methods for their posterior comparison.

2.6.1 *Chemical analysis of LG and PLG*

With the aim of examining the possible effect of the pretreatment on the composition of LG, a proximate chemical analysis of LG and PLG was conducted in accordance with the methods described by the Association of Official Analytical Chemists (AOAC) for the determination of ashes, total proteins, crude fiber, ether extract and humidity (Horwitz and Latimer, 2005; Guerrero-Coronilla *et al*., 2015).

Table 1. Kinetic models of biosorption.

Model	Equation	Parameters	Reference	Eq.
Pseudo-first order	$q_t = q_{eq}\left[1 - e^{(-k_1 t)}\right]$	q_{eq}, k_1	Basha and Murthy, 2007	(3)
Pseudo-second order	$q_t = \dfrac{t}{\left(\frac{1}{k_2 * q_{eq}^2}\right) + \left(\frac{t}{q_{eq}}\right)}$	q_{eq}, k_2	Gupta *et al*., 2019	(4)
Elovich	$q_t = \frac{1}{B}\, ln(AB) + \frac{1}{B}\, ln\, t$	A, B	Gupta *et al*., 2019	(5)
Fractional power	$q_t = k_p t^{\nu}$	k_p, ν	Basha and Murthy, 2007	(6)

The quantity of the extract free of nitrogen (total carbohydrates) was estimated by Eq. 7:

$$\%\text{Extract free of nitrogen} = 100 - \%\text{Ashes} - \%\text{Total proteins} - \%\text{Crude fiber} - \%\text{Ether} \quad (3)$$

The level of humidity was established with a thermobalance (Guerrero-Coronilla *et al*., 2015) in order to make the necessary adjustments to express the results of the proximate chemical analysis as the concentration of the various components of *Lemna gibba* in dry base.

2.6.2 *Pore size and surface area*

The surface area and porosity were assessed on Quantachrome® ASiQwin™ Automated Gas Sorption Data Acquisition and Reduction equipment. The isotherms of adsorption/desorption of gasified liquid nitrogen were recorded while using a vacuum pump at 77 K (the samples were pretreated at 373 K with nitrogen). The surface area was ascertained by multipoint BET (Brunauer, Emett and Teller) and the distribution of pore size by the BJH method (Barret, Joyner and Halenda) (Jacques *et al*., 2007).

2.6.3 *Zeta potential (ζ)*

Flasks were prepared with type II deionized water adjusted to different values of pH (from 1-7) with solutions of HCl and NaOH (0.1 and 0.01 M). Afterwards, a sufficient quantity of LG or PLG was placed in each flask to achieve a 1 mg L^{-1} concentration of biosorbent. The suspensions were evaluated on a zeta Plus ZA apparatus (Bruce and Weiner, 2011).

2.6.4 *Infrared spectroscopy (ATR-FTIR)*

ATR-FTIR images were recorded to verify the changes in PLG with respect to LG, and to elucidate the sites of sorption. With the aim of saturating the binding sites of the biosorbent with the metal, a concentration of 1 g L^{-1} of PLG was put in contact with a solution of 300 mg L^{-1} of Co^{2+} at pH 7.0 and at rt for 2 h under constant shaking at 140 rpm. The saturated biosorbent (PLG-Co) was washed with distilled water and ionized to eliminate the excess metal, and then dried at 60 ºC for 48 h. Representative samples of LG, PLG and PLG-Co were dried at 105 ºC for 24 h and examined on a FTIR Model IR2 Horiba Jobin Yvon spectrophotometer equipped with an ATR crystal diamond objective. The spectra were obtained at a magnification of 36X in the interval of 4000-400 cm^{-1}, with 32 scans and a spectral resolution of 2 cm^{-1}.

3 Results and discussion

The abiotic control did not produce a decrease in the concentration of Co^{2+}. Consequently, the results of the other groups depict the interaction of Co^{2+} with the biosorbent under study.

3.1 *Evaluation of the effect of the pretreatments*

For analysis of the data, the pretreatments of LG were organized in three classifications: a) water at rt and at 60 ºC, neutral salts (NaCl and $MgSO_4$), and organic solvents (acetone and hexane), b) acids and c) alkalis. The kinetics of the biosorption of Co^{2+} is shown in Figure 1 for LG and the plant material with the pretreatments of the first classification.

Among the pretreatments tested in the first classification (Fig. 1), hexane exhibited the greatest biosorption capacity with respect to the control (LG), probably a result of its efficient removal of lipids and pigments (Martínez-Guerra *et al*., 2014; Salazar-Rabago and Leyva-Ramos, 2016). The biosorption capacity was 39% greater for the material pretreated with hexane (26.70 mg g^{-1} vs the control value of 19.17 mg g^{-1}). The pretreatments with water at rt and 60 ºC enhance biosorption by removing impurities on the surface of the biosorbent, thus leading to better availability of the active sites of sorption (Wang and Chen, 2006; Guerrero-Coronilla *et al*., 2015). In the present study, the change in the biosorption capacity found experimentally was not significant in either case, producing an increase of 14.8-18.9% (versus the control).

Regarding the neutral salts, the pretreatment with $MgSO_4$ improved the removal of Co^{2+} (compared to the control), producing a biosorption capacity of 22.46 mg g^{-1}. This is probably because the Mg^{2+} ions substitute the H^+ ions at the sorption site during the preparation of the biosorbent. Subsequently, biosorption is favored by the interaction of exchange of Mg^{2+} by Co^{2+} promoted by the size of the ions, as would happen with an ion exchange resin (Yazici *et al*., 2008; Khosravihaftkhany *et al*., 2015; Dabbagh *et al*., 2016).

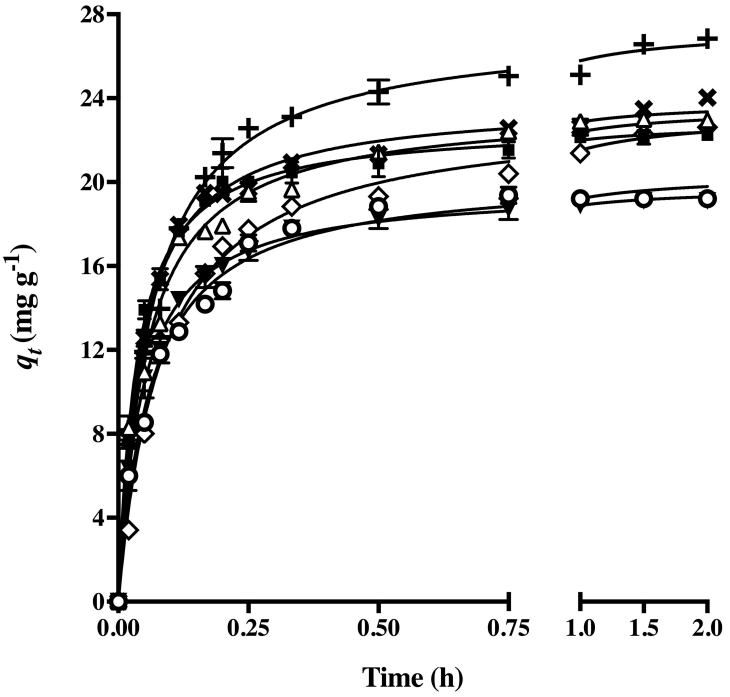

Fig. 1. The kinetics of biosorption of Co^{2+} by untreated *Lemna gibba* (LG) (○)) and the same plant material pretreated with: (■) water at rt, (△) water at 60 ºC, (▼) NaCl (0.1 M), (◊) $MgSO_4$ (0.1 M), (×) acetone (1% v/v) and (+) hexane (1% v/v). The continuous line is the biosorption tendency predicted by the pseudo-second order model.

In some studies, NaCl has improved the removal of divalent ions such as Cu^{2+}, Ni^{2+} and Cd^{2+} (Yazici *et al*., 2008, Khajavian *et al*., 2019), which is attributed to the decreased acidity of the biomass stemming from the substitution of H^+ by Na^+ (Teymouri *et al*., 2013). In the current investigation, however, the effect of NaCl was null, since its q_{e-exp} (18.95 mg g^{-1}) was not significantly different from the value for LG.

The data are expressed as the biosorption capacity at equilibrium (q_{e-exp}), the time necessary to reach equilibrium (t_{eq}), the biosorption capacity at equilibrium predicted by the corresponding model (q_{eq}), the correlation coefficient squared (R^2), and the parameters of the error function of the distinct kinetic models employed (Table 2).

Among all the models herein examined, the pseudo-second order model yielded the highest correlation coefficient (R^2) and the lowest values of SS, Syx and $AICc$. Moreover, the pseudo-second order model predicted values of q_{eq} that are very close to those found experimentally, making it the most adequate model for describing the kinetics of the effects of the pretreatments (with water at different temperatures, with neutral salts and with organic solvents assayed for the biosorption of the sorbate). The continuous line that joins the values in Figure 1 shows the tendency of the kinetics of the pseudo-second order model. The kinetics of LG (the control) and the plant material subjected to the distinct pretreatments with weak acids (KH_2PO_4, NH_4Cl and CH_3COOH) and strong acids (HCl, HNO_3 and H_2SO_4) are shown in Figure 2.

Acid treatments are reported to improve the biosorption capacity of divalent cations since they expose new sites of sorption by eliminating minerals and particles of dust on the cell wall and by protonating the plant cell. They are also capable of increasing porosity, leading to a greater surface area available for biosorption (Khokhar *et al*., 2019).

In the current contribution, pretreatments with weak acids significantly reduced the biosorption capacity (versus the control). Contrarily, the HNO_3 and HCl pretreatments produced a q_{e-exp} of 19.3 mg g^{-1} and 19.26 mg g^{-1}, respectively, which are very close to the control value (19.17 mg g^{-1}).

Table 2. Parameters of the kinetic model of biosorption of Co^{2+} by untreated *Lemna gibba* (LG) and the same plant material submitted to pretreatment with water at different temperatures, neutral salts and organic solvents.

	LG	H_2O RT	H_2O 60 °C	NaCl 0.1 M	$MgSO_4$ 0.1 M	C_3H_6O 1%	C_6H_{14} 1%
t_{eq} (h)	0.5	0.75	0.75	0.75	1.5	1.5	1.5
$q_{e\text{-}exp}$ (mg g^{-1})	19.17 ± 0.09	22.01 ± 0.16	22.81 ± 0.14	18.95 ± 0.09	22.46 ± 0.16	23.76 0.27	26.70 ± 0.14
Pseudo-first order							
q_{eq} (mg g^{-1})	18.76 ± 0.21	21.13 ± 0.17	21.66 ± 0.30	18.23 ± 0.19	20.97 ± 0.21	21.95 ± 0.23	25.06 ± 0.27
k_1 (h^{-1})	10.56 ± 0.48	18.06 ± 0.72	12.56 ± 0.73	14.39 ± 0.67	8.791 ± 0.33	15.39 ± 0.75	10.88 ± 0.47
R^2	0.9674	0.9784	0.9478	0.9680	0.9791	0.9664	0.9705
SS	59.28	46.89	122.6	52.86	53.75	80.74	95.94
Syx	1.048	0.9318	1.507	0.9894	0.9977	1.223	1.333
AICc	9.648	-3.482	50.33	3.229	4.164	26.95	36.61
Pseudo-second order							
q_{eq} (mg g^{-1})	20.40 ± 0.18	22.77 ± 0.11	23.57 ± 0.21	19.73 ± 0.11	23.33 ± 0.17	23.85 ± 0.12	27.38 ± 0.20
k_2 (g mg^{-1} h^{-1})	0.794 ± 0.04	1.242 ± 0.04	0.811 ± 0.04	1.135 ± 0.04	0.508 ± 0.02	0.968 ± 0.03	0.590 ± 0.02
R^2	0.9873	0.9942	0.9848	0.9931	0.9927	0.9946	0.9910
SS	23.00	12.55	35.60	11.46	18.68	12.86	29.18
Syx	0.6527	0.4822	0.8120	0.4606	0.5881	0.4880	0.7352
AICc	-43.37	-77.27	-18.90	-82.40	-55.03	-75.94	-30.03
Elovich							
A (mg g^{-1} h^{-1})	1647 ± 320.2	7522 ± 2691	2792 ± 523.9	3322 ± 847	845.7 ± 100.9	4093 ± 932.8	2145 ± 359.9
B (g mg^{-1})	0.323 ± 0.02	0.350 ± 0.02	0.294 ± 0.01	0.369 ± 0.02	0.244 ± 0.009	0.304 ± 0.01	0.238 ± 0.009
R^2	0.9013	0.8352	0.9222	0.8830	0.9376	0.9048	0.9234
SS	93.53	143.3	86.43	86.57	98.84	100.8	129.5
Syx	1.368	1.693	1.315	1.316	1.406	1.420	1.610
AICc	37.03	59.22	32.92	33.00	39.90	40.94	53.96
Fractional power							
k_p (mg g^{-1} h^{-v})	19.15 ± 0.37	22.22 ± 0.41	22.53 ± 0.35	19.02 ± 0.34	21.35 ± 0.44	23.13 ± 0.37	25.78 ± 0.45
v (h^{-1})	0.187 ± 0.01	0.140 ± 0.01	0.175 ± 0.01	0.160 ± 0.01	0.229 ± 0.01	0.161 ± 0.01	0.190 ± 0.01
R^2	0.8219	0.7582	0.8572	0.8055	0.8443	0.8331	0.8500
SS	168.8	210.3	158.7	143.9	246.8	176.9	253.6
Syx	1.837	2.051	1.781	1.697	2.221	1.881	2.252
AICc	67.72	79.16	64.51	59.43	87.47	70.15	88.90

t_{eq}, time required to reach equilibrium; q_{e-exp}, experimental biosorption capacity at equilibrium; q_{eq}, the predicted biosorption capacity at equilibrium; k_1, constant of the velocity of sorption of the pseudo-first order model (min^{-1}); R^2, the correlation coefficient squared; SS, sum of the squares; Syx, standard deviation of the residuals; $AICc$, corrected Akaike information criterion; k_2, constant of the velocity of sorption of the pseudo-second order model (g mg^{-1} min^{-1}); A, initial velocity of adsorption (mg g^{-1} h^{-1}); B, constant related to the coverage of the surface and the activation energy for chemisorption (mg g^{-1}); k_p, constant of the fractional power model (mg g^{-1} h^{-v}); v, constant of velocity (h^{-1}).

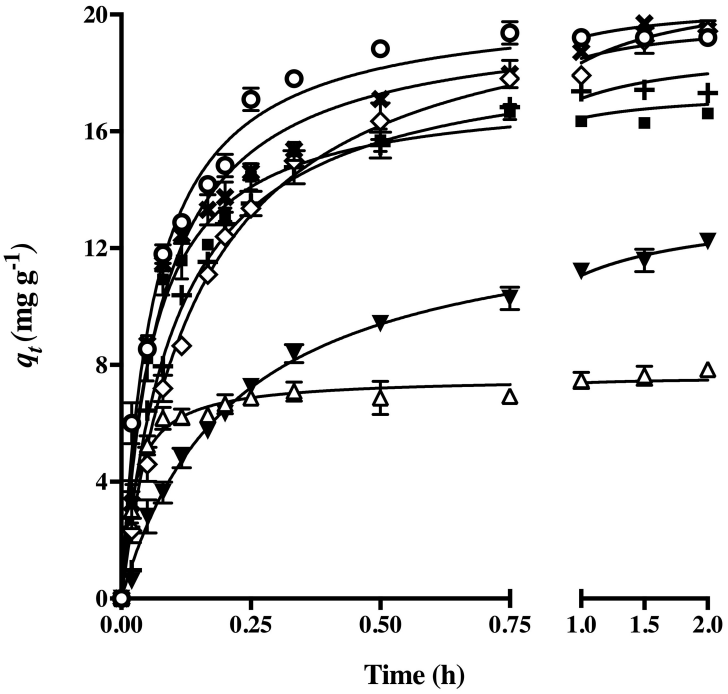

Fig. 2. The kinetics of biosorption of Co^{2+} by untreated *Lemna gibba* (LG) (○) and the same plant material pretreated with 0.1 M of the following acids: (■) KH_2PO_4, (△) NH_4Cl, (▼) CH_3COOH, (◊) HCl, (×) HNO_3, and (+) H_2SO_4. The continuous line is the biosorption tendency predicted by the pseudo-second order model.

However, when comparing the t_{eq} of LG to the value for the biosorbent pretreated with HCl or HNO_3, the latter pretreatments both exhibited a two- to three-fold increase in the time required to reach equilibrium. The negative effect of the acids probably stems from their protonation of the functional groups of the cell wall of *Lemna gibba* and the consequent decrease in the electronegativity of the cell surface and removal velocity of Co^{2+} (Dabbagh *et al.*, 2016). Unlike HCl and HNO_3, the H_2SO_4 pretreatment caused a lower biosorption (q_{e-exp}) versus the control (LG). The same phenomenon has been observed in other studies (Javaid *et al.*, 2011) and has been attributed to the fact that this acid is a strong oxidizing and dehydrating agent capable of damaging the structure of the biosorbent (Abdolali *et al.*, 2015).

The experimental results of the acid pretreatments are depicted in Table 3, expressed as the experimental biosorption capacity at equilibrium (q_{e-exp}), the time necessary to reach equilibrium (t_{eq}), the biosorption capacity predicted by the corresponding model (q_{eq}), the constants for each of the models ($qe, k1, k2, A, B, kp$ and v), the correlation coefficient (R^2), and the error functions (SS, Syx and $AICc$). As with the previous pretreatments, the equation for the pseudo-second order model was the one with the highest correlation coefficient (R^2) and the lowest error functions. Additionally, the values of biosorption capacity at the predicted equilibrium are very close to those found experimentally. Hence, the pseudo-second order model was adequate for describing the kinetics of biosorption of Co^{2+} by LG and by *Lemna gibba* pretreated with the tested acids. The continuous lines joining the values in Figure 2 illustrates the predicted biosorption afforded by the pseudo-second order kinetic model.

The results of the kinetics of untreated LG and the same plant material pretreated with weak (K_2HPO_4, $NaHCO_3$ and Na_2CO_3) and strong alkaline solutions (NaOH and KOH) are shown in Figure 3.

All the pretreatments with alkaline solutions increased the capacity of biosorption of Co^{2+} by *Lemna gibba*. The best capacity of removal of Co^{2+} was 30.67 mg g^{-1}, achieved with the K_2HPO_4 (0.1 M) pretreatment.

Table 3. Parameters of the kinetic models of biosorption of Co^{2+} by untreated *Lemna gibba* (LG) and the same plant material submitted to pretreatment with acids.

	LG	KH_2PO_4 0.1 M	NH_4Cl 0.1 M	CH_3COOH 0.1 M	HCl 0.1 M	HNO_3 0.1 M	H_2SO_4 0.1 M
t_{eq} (h)	0.5	0.75	1.0	1.5	1.5	1.0	0.75
$q_{e\text{-}exp}$ (mg g^{-1})	19.17 ± 0.09	16.48 ± 0.09	7.648 ± 0.11	11.90 ± 0.32	19.26 ± 0.16	19.30 ± 0.29	17.23 ± 0.14
Pseudo-first order							
q_{eq} (mg g^{-1})	18.76 ± 0.21	15.93 ± 0.18	7.063 ± 0.08	11.45 ± 0.13	18.46 ± 0.14	17.95 ± 0.28	16.88 ± 0.17
k_1 (h^{-1})	10.56 ± 0.48	11.53 ± 000.53	25.49 ± 1.76	4.102 ± 0.14	5.4 ± 0.13	9.543 ± 0.57	7.3 ± 0.25
R^2	0.9674	0.9700	0.9447	0.9847	0.9912	0.9457	0.9834
SS	59.28	42.03	13.04	12.85	18.69	98.89	29.70
Syx	1.048	0.8822	0.4913	0.4878	0.5882	1.353	0.7417
AICc	9.648	-9.611	-75.16	-75.98	-55.01	38.31	-29.05
Pseudo-second order							
q_{eq} (mg g^{-1})	20.40 ± 0.18	17.42 ± 0.17	7.574 ± 0.08	13.44 ± 0.14	21.14 ± 0.16	19.89 ± 0.21	18.91 ± 0.22
k_2 (g mg^{-1} h^{-1})	0.794 ± 0.04	0.972 ± 0.05	5.188 ± 0.44	0.345 ± 0.01	0.309 ± 0.01	0.665 ± 0.04	0.505 ± 0.03
R^2	0.9873	0.9839	0.9655	0.9933	0.9952	0.9846	0.9858
SS	23.00	22.52	8.136	5.614	10.20	28.12	25.50
Syx	0.6527	0.6458	0.3882	0.3224	0.4345	0.7216	0.6871
AICc	-43.37	-44.54	-101.6	-122.3	-88.93	-32.12	-37.60
Elovich							
A (mg g^{-1} h^{-1})	1647 ± 320.2	1282 ± 283.7	7740 ± 4104	153.0 ± 5.55	349.3 ± 21.9	894.0 ± 101.5	459.1 ± 50.55
B (g mg^{-1})	0.323 ± 0.01	0.367 ± 0.02	1.203 ± 0.09	0.374 ± 0.006	0.245 ± 0.006	0.297 ± 0.009	0.282 ± 0.01
R^2	0.9013	0.8695	0.7735	0.9860	0.9692	0.9500	0.9304
SS	93.53	99.05	17.99	9.032	47.02	53.06	84.09
Syx	1.368	1.407	0.5999	0.4250	0.9698	1.030	1.297
AICc	37.03	40.01	-48.69	-84.52	1.267	7.548	31.50
Fractional power							
k_p (mg g^{-1} $h^{-\nu}$)	19.15 ± 0.37	16.44 ± 0.37	7.535 ± 0.13	10.59 ± 0.19	17.76 ± 0.36	18.50 ± 0.33	16.80 ± 0.41
ν (h^{-1})	0.187 ± 0.01	0.187 ± 0.02	0.121 ± 0.01	0.349 ± 0.02	0.298 ± 0.02	0.22 ± 0.01	0.253 ± 0.02
R^2	0.8219	0.7742	0.7198	0.9209	0.8880	0.8721	0.8180
SS	168.8	171.4	22.27	51.04	171.2	135.9	219.8
Syx	1.837	1.851	0.6673	1.010	1.850	1.648	2.097
AICc	67.72	68.51	-37.60	5.534	68.46	56.44	81.46

t_{eq}, time required to reach equilibrium; q_{e-exp}, experimental biosorption capacity at equilibrium; q_{eq}, the predicted biosorption capacity at equilibrium; k_1, constant of the velocity of sorption of the pseudo-first order model (min^{-1}); R^2, the correlation coefficient squared; SS, sum of the squares; Syx, standard deviation of the residuals; $AICc$, corrected Akaike information criterion; k_2, constant of the velocity of sorption of the pseudo-second order model (g mg^{-1} min^{-1}); A, initial velocity of adsorption (mg g^{-1} h^{-1}); B, constant related to the coverage of the surface and the activation energy for chemisorption (mg g^{-1}); k_p, constant of the fractional power model (mg g^{-1} $h^{-\nu}$); ν, constant of velocity (h^{-1}).

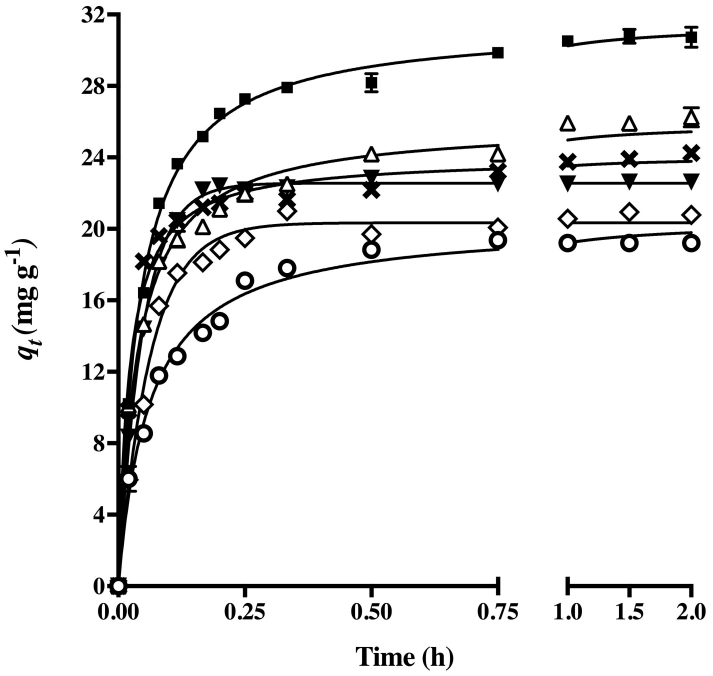

Fig. 3. Kinetics of the biosorption of Co^{2+} by untreated *Lemna gibba* (LG) (○) and the same plant material pretreated with 0.1 M of the following alkalis: (■) K_2HPO_4, (△) $NaHCO_3$, (▼) Na_2CO_3, (◊) NaOH, and (×) KOH. The continuous line is the biosorption tendency predicted by the pseudo-second order model.

This value was 60% greater than that found with untreated LG. Alkaline pretreatments are usually beneficial to biosorption since they are capable of breaking the cell wall. They help to remove tannins, chlorophyll, lipids, proteins and lignin, which enables a better exposure of the active sites and generates new sites. Additionally, they negatively charge the biosorbent cell surface, thus attracting the positively charged Co^{2+} to the sorption sites. These factors all lead to an enhanced uptake capacity of the biosorbent for the sorbate (Yazici *et al*., 2008; Argun *et al*., 2009; Suazo-Madrid *et al*., 2011; Ighalo and Adeniyi, 2020).

The pretreatments of plant leaves with NaOH and $NaHCO_3$ for the removal of heavy metals are popular and effective (Adeniyi and Ighalo, 2019). NaOH has been reported as a pretreatment particularly capable of improving the capacity of plant material to remove Co^{2+} (Nadeem *et al*., 2014; Singh and Shukla, 2015). In the current study, there was a clear positive effect on the sorption capacity of *Lemna gibba* produced by alkaline solutions, especially with $NaHCO_3$ and K_2HPO_4. The latter turned out to be the best option. The experimental capacity of biosorption at equilibrium (q_{e-exp}), the biosorption capacity predicted by the corresponding model (q_{eq}), the time necessary to reach equilibrium (t_{eq}), the parameters of kinetics, and the error functions for the alkali pretreatments are included in Table 4. The pseudo-second order equation predicted a capacity of equilibrium near the experimental value, as well as yielding the highest correlation coefficient (R^2) and the lowest error values compared to all the other models assayed. The continuous line represents the predicted kinetics of biosorption of LG and the same plant material subjected to alkali pretreatments, according to the pseudo-second order model (Fig. 3).

Among the 17 pretreatments carried out, the greatest increase in biosorption capacity with respect to the control (19.17 mg g^{-1}) was obtained with sodium bicarbonate (26.03 mg g^{-1}), hexane (26.7 mg g^{-1}) and K_2HPO_4 (30.67 mg g^{-1}). Besides the maximum sorption capacity, there was another important factor involved in the selection of the most appropriate pretreatment, being the time necessary to reach equilibrium.

Table 4. Parameters of the kinetic models of biosorption of Co^{2+} by untreated *Lemna gibba* (LG) and the same plant material submitted to pretreatment with alkalis.

	LG	K_2HPO_4 0.1 M	$NaHCO_3$ 0.1 M	Na_2CO_3 0.1 M	NaOH 0.1 M	KOH 0.1 M
t_{eq} (h)	0.5	1.0	1.0	0.25	1.0	1.0
$q_{e\text{-}exp}$ (mg g^{-1})	19.17 ± 0.09	30.67 ± 0.08	26.03 ± 0.11	22.51 ± 0.08	20.76 ± 0.11	23.97 ± 0.14
Pseudo-first order						
q_{eq} (mg g^{-1})	18.76 ± 0.21	29.07 ± 0.25	23.90 ± 0.32	22.56 ± 0.05	20.34 ± 0.12	22.54 ± 0.17
k_1 (h^{-1})	10.56 ± 0.48	15.86 ± 0.65	17.50 ± 1.15	20.86 ± 0.26	15.86 ± 0.45	28.54 ± 1.34
R^2	0.9674	0.9766	0.9398	0.9980	0.9894	0.9751
SS	59.28	97.73	164.8	4.740	22.91	57.20
Syx	1.048	1.345	1.747	0.2963	0.6513	1.029
AICc	9.648	37.65	66.91	-131.8	-43.59	7.653
Pseudo-second order						
q_{eq} (mg g^{-1})	20.40 ± 0.18	31.49 ± 0.12	25.91 ± 0.17	24.01 ± 0.22	21.96 ± 0.24	24.04 ± 0.16
k_2 (g mg^{-1} h^{-1})	0.794 ± 0.04	0.769 ± 0.2	1.023 ± 0.04	1.464 ± 0.09	1.115 ± 0.08	1.875 ± 0.10
R^2	0.9873	0.9969	0.9898	0.9783	0.9748	0.9859
SS	23.00	13.05	27.96	52.81	54.38	32.42
Syx	0.6527	0.4917	0.7196	0.9889	1.004	0.7748
AICc	-43.37	-75.09	-32.44	3.173	4.820	-24.15
Elovich						
A (mg g^{-1} h^{-1})	1647 ± 320.2	6376 ± 1749	6732 ± 1331	23848 ± 16545	4612 ± 1950	51786 ± 31247
B (g mg^{-1})	0.323 ± 0.01	0.236 ± 0.01	0.296 ± 0.01	0.384 ± 0.04	0.342 ± 0.03	0.413 ± 0.03
R^2	0.9013	0.8760	0.9377	0.6651	0.7515	0.7673
SS	93.53	224.8	67.22	303.0	250.8	158.0
Syx	1.368	2.120	1.159	2.462	2.240	1.778
AICc	37.03	82.62	19.85	98.15	88.33	64.29
Fractional power						
k_p (mg g^{-1} h^{-v})	19.15 ± 0.37	30.51 ± 0.54	25.42 ± 0.32	23.39 ± 0.55	21.12 ± 0.52	23.93 ± 0.39
v (h^{-1})	0.187 ± 0.01	0.154 ± 0.01	0.152 ± 0.008	0.115 ± 0.01	0.148 ± 0.02	0.108 ± 0.01
R^2	0.8219	0.7981	0.8805	0.5884	0.6619	0.7098
SS	168.8	365.9	128.9	372.5	341.3	197.1
Syx	1.837	2.705	1.606	2.730	2.613	1.985
AICc	67.72	108.0	53.72	108.9	104.3	75.78

t_{eq}, time required to reach equilibrium; q_{e-exp}, experimental biosorption capacity at equilibrium; q_{eq}, the predicted biosorption capacity at equilibrium; k_1, constant of the velocity of sorption of the pseudo-first order model (min^{-1}); R^2, the correlation coefficient squared; SS, sum of the squares; Syx, standard deviation of the residuals; $AICc$, corrected Akaike information criterion; k_2, constant of the velocity of sorption of the pseudo-second order model (g mg^{-1} min^{-1}); A, initial velocity of adsorption (mg g^{-1} h^{-1}); B, constant related to the coverage of the surface and the activation energy for chemisorption (mg g^{-1}); k_p, constant of the fractional power model (mg g^{-1} h^{-v}); v, constant of velocity (h^{-1}).

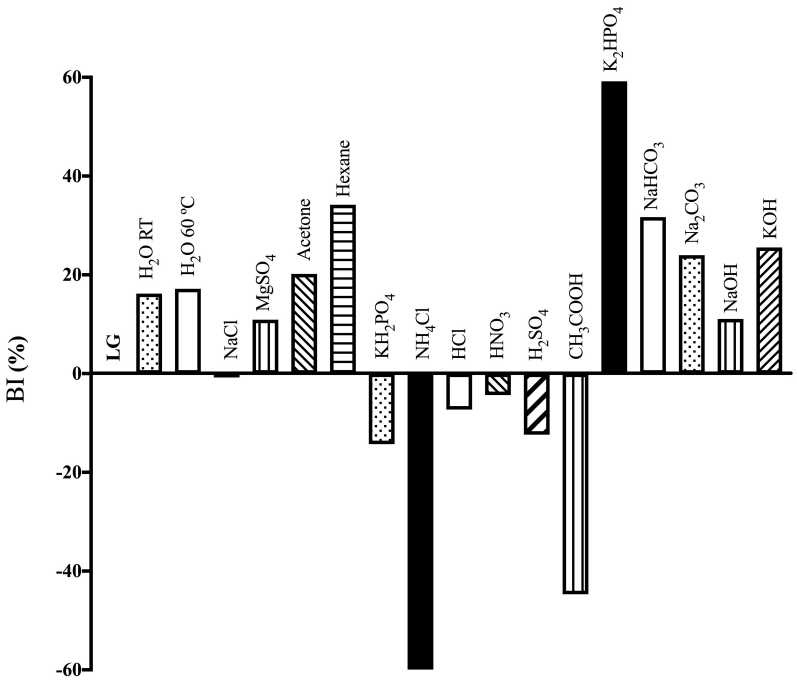

Fig. 4. The behavior index (BI) of the pretreatments tested for their possible improvement of the biosorption of Co^{2+} by *Lemna gibba*, with the untreated plant material serving as the control (0%).

Hence, the BI of the pretreatments was calculated because it portrays the overall behavior of biosorption and thus allows for a more objective evaluation (Fig. 4). The BI revealed that NaCl (0.1 M) had a null effect on the capacity of *Lemna gibba* to remove Co^{2+}. The sharpest decline in biosorption was produced by ammonium chloride (0.1 M). On the other hand, the most advantageous pretreatments were the following (in decreasing order): K_2HPO_4 >> hexane ≈ $NaHCO_3$ > KOH ≈ Na_2CO_3. Based on the aforementioned analysis, K_2HPO_4 (0.1 M) was selected as the best pretreatment of LG for the removal of Co^{2+}, as it significantly improved the uptake capacity of the plant material for the heavy metal. To our knowledge, this is the first report on the pretreatment of a biosorbent with K_2HPO_4.

3.2 Determination of the best concentration of K_2HPO_4 for pretreating Lemna gibba

Distinct concentrations of K_2HPO_4 were tested to attempt to further enhance the capacity of *Lemna gibba* for the removal of Co^{2+}, evaluating the kinetics of each one compared to the control (LG; Fig. 5). Each increment in the concentration of K_2HPO_4 produced a better capacity of removal of Co^{2+} by *Lemna gibba* (Fig. 5). The improvement in biosorption resulting from K_2HPO_4 pretreatment was possibly due to intensifying the degree of dissociation of the functional groups on the cell surface. This type of pretreatment also negatively charges the surface of the biosorbent, which favors the approach of metal ions with a positive charge such as Co^{2+}, thus enhancing the biosorption capacity (Bulgariu and Bulgariu, 2016). In the current contribution, the biosorption capacity of the biomaterial at equilibrium increased 109.3% and 112.8% (versus the control) by pretreating LG with 0.3 M and 0.4 M of K_2HPO_4 in solution, respectively.

Although the greatest biosorption capacity was obtained with K_2HPO_4 at 0.4 M, the statistical analyses with two-way ANOVA and the Tukey test of multiple comparisons indicated a lack of a significant difference between the pretreatments with 0.3 and 0.4 M of K_2HPO_4 ($p>0.05$) in relation to the experimental sorption capacity at equilibrium (q_{e-exp}), the time necessary to reach equilibrium (t_{eq}), and the BI (Fig. 6).

Table 5. Parameters of the kinetic models of biosorption of Co^{2+} by untreated *Lemna gibba* and the same plant material pretreated with different concentrations of K_2HPO_4.

	LG	K_2HPO_4				
		0.05 M	**0.1 M**	**0.2 M**	**0.3 M**	**0.4 M**
t_{eq} **(h)**	0.5	1.0	1.0	0.5	0.5	0.5
$q_{e\text{-}exp}$ **(mg g^{-1})**	19.17 ± 0.09	23.96 ± 0.25	30.67 ± 0.08	34.17 ± 0.25	40.13 ± 0.18	40.80 ± 0.55
Pseudo-first order						
q_{eq} **(mg g^{-1})**	18.76 ± 0.21	23.20 ± 0.22	29.07 ± 0.25	33.05 ±0.27	38.80 ± 0.26	39.35 ± 0.34
k_1 **(h^{-1})**	10.56 ± 0.48	11.36 ± 0.44	15.86 ± 0.65	18.16 ± 0.77	34.96 ± 1.59	29.40 ± 1.63
R^2	0.9674	0.9773	0.9766	0.9754	0.9777	0.9641
SS	59.28	64.34	97.73	127.7	139.4	238.5
Syx	1.048	1.092	1.345	1.538	1.607	2.101
AICc	9.648	14.23	37.65	52.61	57.55	87.60
Pseudo-second order						
q_{eq} **(mg g^{-1})**	20.40 ± 0.18	25.31 ± 0.22	31.49 ± 0.12	35.55 ± 0.10	40.86 ± 0.09	41.70 ± 0.19
k_2 **(g mg^{-1} h^{-1})**	0.794 ± 0.04	0.669 ± 0.03	0.769 ± 0.02	0.813 ± 0.01	1.503 ± 0.03	1.199 ± 0.04
R^2	0.9873	0.9869	0.9969	0.9980	0.9980	0.9936
SS	23.00	37.15	13.05	10.12	12.31	42.65
Syx	0.6527	0.8294	0.4917	0.4329	0.4775	0.8887
AICc	-43.37	-16.52	-75.09	-89.35	-78.37	-8.790
Elovich						
A **(mg g^{-1} h^{-1})**	1647 ± 320.2	2170 ± 471.8	6376 ± 1749	13245 ± 4518	754937 ± 572134	177025 ± 97378
B **(g mg^{-1})**	0.323 ± 0.01	0.262 ± 0.01	0.237 ± 0.01	0.228 ± 0.01	0.300 ± 0.02	0.256 ± 0.02
R^2	0.9013	0.8826	0.8760	0.8537	0.7797	0.8264
SS	93.53	172.7	224.8	293.2	279.1	285.5
Syx	1.368	1.859	2.120	2.421	2.363	2.390
AICc	37.03	68.93	82.62	96.43	93.87	95.06
Fractional power						
k_p **(mg g^{-1} h$^{-\nu}$)**	19.15 ± 0.37	23.85 ± 0.48	30.51 ± 0.54	34.73 ± 0.59	40.85 ± 0.52	41.64 ±0.54
ν **(h^{-1})**	0.187 ± 0.01	0.184 ± 0.01	0.155 ± 0.01	0.139 ± 0.01	0.086 ± 0.007	0.101 ± 0.008
R^2	0.8219	0.8002	0.7981	0.7788	0.7293	0.7740
SS	168.8	294.1	365.9	443.3	342.9	371.8
Syx	1.837	2.425	2.705	2.978	2.619	2.727
AICc	67.72	96.59	108.0	117.9	104.6	108.8

t_{eq}, time required to reach equilibrium; q_{e-exp}, experimental biosorption capacity at equilibrium; q_{eq}, the predicted biosorption capacity at equilibrium; k_1, constant of the velocity of sorption of the pseudo-first order model (min^{-1}); R^2, the correlation coefficient squared; SS, sum of the squares; Syx, standard deviation of the residuals; $AICc$, corrected Akaike information criterion; k_2, constant of the velocity of sorption of the pseudo-second order model (g mg^{-1} min^{-1}); A, initial velocity of adsorption (mg g^{-1} h^{-1}); B, constant related to the coverage of the surface and the activation energy for chemisorption (mg g^{-1}); k_p, constant of the fractional power model (mg g^{-1} h$^{-\nu}$); ν, constant of velocity (h^{-1}).

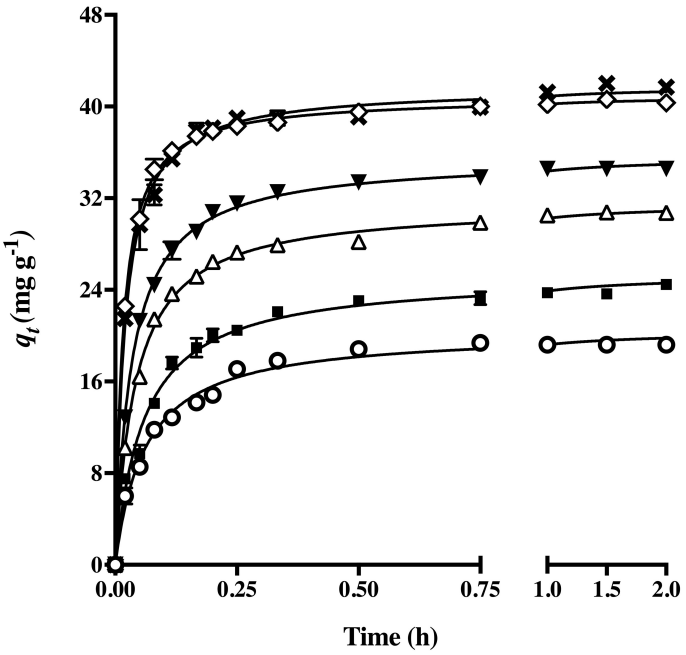

Fig. 5. Kinetics of the biosorption of Co^{2+} by untreated *Lemna gibba* (control) (○) and the pretreatment of the same plant material with K_2HPO_4 at various concentrations: (■) 0.05 M, (△) 0.1 M, (▼) 0.2 M, (◊) 0.3 M, and (×) 0.4 M. The continuous line is the predicted biosorption tendency of the pseudo-second order model.

Consequently, there was no justification for the use of the 0.4 M concentration and the K_2HPO_4 pretreatment at 0.3 M (denominated PLG) was selected as the best for the biosorption of Co^{2+} by *Lemna gibba*.

The experimental kinetics of sorption (q_{e-exp}), the time necessary to reach equilibrium (t_{eq}), the biosorption capacity predicted by the corresponding model (q_{eq}), the constants for each of the models, the correlation coefficient (R^2), and the error functions for each of the models tested are shown in Table 5. Similar to the previous results, the pseudo-second order model afforded the highest correlation coefficient (R^2) and the lowest error functions.

3.3 Characterization of the biosorbent

3.3.1 Proximate chemical analysis of the biosorbent

In order to evaluate the possible changes in the composition of the biosorbent due to the selected pretreatment, a proximate chemical analysis of *Lemna gibba* was carried out on the untreated plant material (LG) and that treated with K_2HPO_4 at 0.3 M (PLG) (Table 6). The percentage of humidity of the biosorbent was 5.90% without pretreatment and 5.06% with pretreatment.

According to the analysis, LG contains a small amount of ether extract (4.92%) and a high quantity of protein (20.97%). Azer (2013) observed that swollen duckweed, being a rich source of amino acids, serves as feed for poultry, pigs and cows in diverse regions. The elevated ash content (24.47%) is related to the quantity of minerals present in the plant, including magnesium, silicon, sodium, potassium and sulfur (Landolt and Kandeler, 1987). Crude fiber and the nitrogen-free extract correspond to carbohydrates. More specifically, crude fiber refers to the content of cellulose, hemicellulose and lignin, characteristic of the cell wall of plants. The nitrogen-free content corresponds to digestible carbohydrates and non-nitrogenated soluble organic solvents (Zhao *et al.*, 2014). Based on the proximate chemical analysis of PLG and LG, the pretreatment did not significantly change the concentration of proteins. The content of lipids was diminished by the pretreatment, but the original concentration was already very small.

Table 6. Proximate chemical analysis of LG and PLG in dry base.

Biosorbent	LG	PLG
% Ether extract	4.92	3.91
% Crude fiber	11.17	19.05
% Protein	20.97	20.44
% Ash	24.47	17.88
% Nitrogen-free extract	38.47	38.72

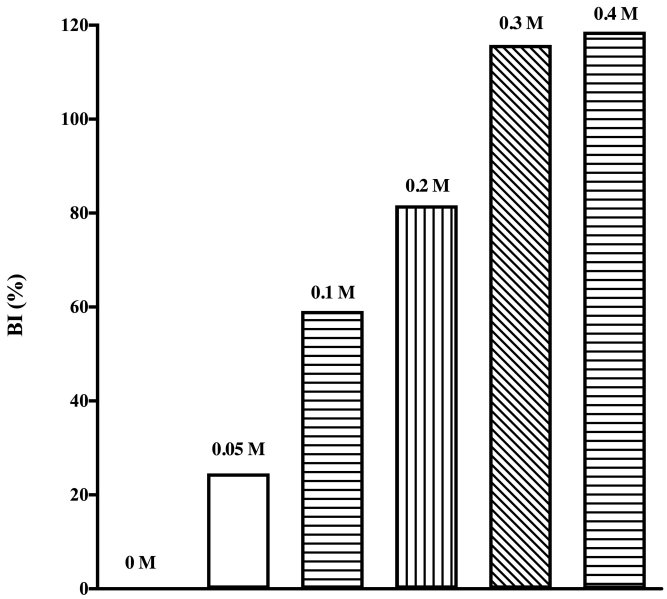

Fig. 6. Behavior index (*BI*) of the biosorption of Co^{2+} by *Lemna gibba* after pretreatment with distinct concentrations of K_2HPO_4 (versus the untreated plant material).

The important differences in the composition of LG an PLG are the 26.9% reduction in the percentage of ash and the increase from 11.17% to 19.05% in crude fiber. As can be appreciated, pretreatment with 0.3 M of K_2HPO_4 had a definite effect on the composition of the biosorbent, removing ash and increasing the relative concentration of cellulose, hemicellulose and lignin, according to the AOAC methods used (Horwitz and Latimer, 2005). Such a change enhanced the exposure of the active sites on the surface of *Lemna gibba* and consequently its uptake capacity for Co^{2+}.

3.3.2 Pore size and surface area

The pore size and surface area of LG and PLG are shown in Table 7. Due to the size of the pores found, both materials are classified as mesoporous (2 nm-20 nm) (El-Sayed and Nada, 2017).

Surface area and porosity affect the biosorption of sorbates. However, no relation exists between the volume or diameter of a pore on a particular surface and the capacity of removal of heavy metals by a pretreated biosorbent (Martín-Lara *et al*., 2013; Patel and Vashi, 2013; Abdelwahab *et al*., 2015). In the current study, there was no significant difference in the volume of the pores between LG and PLG. The pretreatment increased the pore size of the biosorbent and decreased the specific surface available for biosorption, with a net effect of an improved capacity of removal of Co^{2+}. Similar qualitative results were obtained by El-Sayed and Nada (2017) in regard to the treatment of oil palm leaves with polyethylenimine for the biosorption of Pb^{2+} and Cr^{6+}. This indicates that the surface area of the material is not the only factor to consider for predicting the capacity of a biosorbent to remove a contaminant from an aqueous solution.

Table 7. Surface area of LG an PLG as well as their pore volume and diameter.

Material	Surface area ($m^2\ g^{-1}$)	Pore volume ($cm^3\ g^{-1}$)	Pore diameter (nm)
LG	1.826	0.006	2.125
PLG	1.332	0.006	3.277

3.3.3 Zeta potential (ζ)

The zeta potential (ζ) is one of the most useful parameters for characterizing the surface charge of materials. It is defined as the charge on the interface between the solid surface and the liquid medium (Bruce and Weiner, 2011). The difference in the zeta potential between LG and PLG at distinct pH values can be seen in Figure 7. The pH for each material at zero charge (a zeta potential of 0, or an isoelectric point (ζ_0) of 0) is depicted for each material.

In the case of LG, the pH values of 1 and 2 resulted in a positive zeta potential (a positive surface charge). At a point above the latter pH value, the zeta potential reached zero (ζ_0 LG= 2.37). Hence, the zeta potential of LG decreased in value as the pH increased, providing a biosorbent with a progressively more negative surface charge as the pH approached 7. At the latter pH, the surface of the biosorbent had the largest quantity of negatively charged sites, and therefore the greatest potential of interaction with the Co^{2+} ions by means of electrostatic attraction.

Cellulose, one of the main components in the structure of plants, has a negative zeta potential at a pH above 3 (Myśliwiec *et al*., 2016). Similarly, diverse studies on plants have reported a ζ_0 between pH 2 and 4 (Schneider *et al*., 2001; Gupta *et al*., 2019). The negative charge of the biosorbent could be due to the ionization of the -OH groups of cellulose (Pei *et al*., 2019) and of the carboxyl groups present in other components (Schneider *et al*., 2001). The pretreatment caused a slight decline in the pH level corresponding to a 0 charge of the biosorbent (ζ_0 PLG =1.62) and reduced the zeta potential of the cell surfaces of the plant material (PLG<LG), indicating that the pretreatment increased the electronegativity of the surface of the biosorbent, which improved the uptake capacity for Co^{2+} ions.

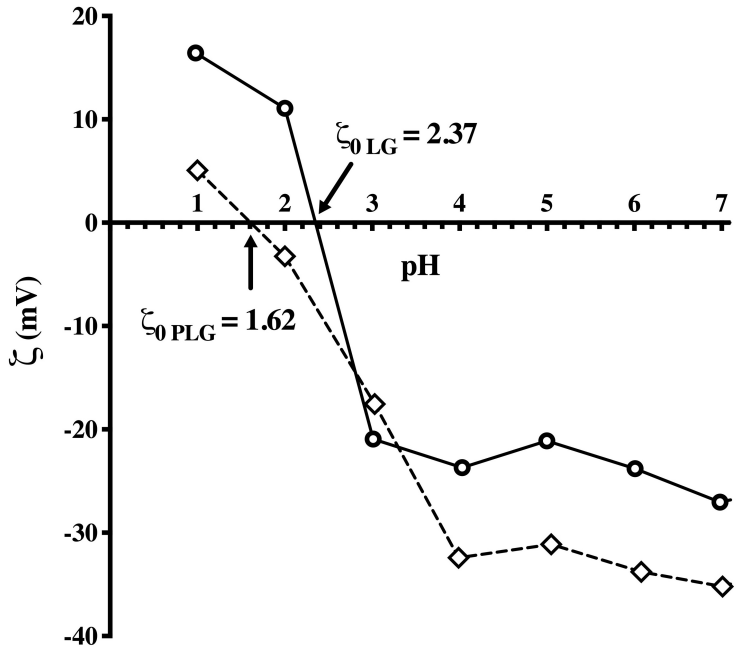

Fig. 7. Zeta potential (ζ) of (○) LG and (◊) PLG at distinct pH values.

3.3.4 Fourier-transform infrared (FTIR) spectroscopy

FTIR spectroscopy was employed to elucidate the main pretreatment-induced changes in the functional groups of the biosorbent and the probable sites of sorption of Co^{2+} by PLG. Hence, images were recorded for LG, PLG and PLG loaded with Co^{2+} (PLG-Co). The main frequencies detected in the corresponding spectra and their possible assignment can be appreciated in Figure 8 and Table 8.

The FTIR spectra of LG (Fig. 8) shows a well-defined moderate band at around 3310.5 cm^{-1}, resulting from the vibration of the amine (N-H) and hydroxyl (O-H) groups. Bands also appeared at 1722.2 cm^{-1}, characteristic of the carboxyl groups that are common in the cell wall, and at 1610 cm^{-1} and 1513 cm^{-1}, typical of the amide groups of proteins. The bands below 800 cm^{-1} belong to the fingerprint of LG (Saygideger *et al*., 2005). After the pretreatment, the FTIR spectrum of PLG (Fig. 8) displayed a broader and more definite band (compared to the spectrum of LG) at around 3200 cm^{-1}, indicating more numerous -OH and -NH groups. The likely explanation is that the treatment removes some ions bound to these functional groups, which is in agreement with the proximate chemical analysis. The analysis showed a lower quantity of ash with the 0.3 M K_2HPO_4 treatment. Another change observed was in the displacement of the amide group from 1610 cm^{-1} to 1629 cm^{-1} and from 1513 cm^{-1} to 1532 cm^{-1}.

Moreover, the FTIR spectrum verified a modification in the frequency of the bending of the carboxylic group at 1725.6 cm^{-1}. The very notable peak in LG was a small band in PLG. Under the basic conditions of treatment (pH=9), the carboxyl group may have become carboxylic ($-COO^-$) (Rakhshaee *et al*., 2009), causing the vibration of the group to decrease.

Table 8. Vibration frequencies in the FTIR spectra of LG, PLG and PLG-Co and their corresponding assignments.

Frequency (cm^{-1})			Assignment	Reference
LG	**PLG**	**PLG-Co**		
3310	3269.6	3271.4	Vibration: -OH and -NH	Tang *et al*., 2013
2916	2923.6	2919.9	Extension of CH_2	Dos Santos Lima *et al*., 2011 Bayramoglu *et al*., 2013
1722.2	1725.6	1729.3	Extension of C=O in COOH	Li *et al*., 2011 Tang *et al*., 2013
1610.6	1629.2	1605	Extension of N-H and C=O of the amide group	Giri and Patel, 2012
1513	1532.5	ND	N-H bend C-N peptide bond of the proteins	Bayramoglu *et al*., 2013 Dos Santos Lima *et al*., 2011
1450	1406	1413	Extension of O-H and C=O in COOH	Dos Santos Lima *et al*., 2011
1411	1380	1363.2	Movement of $-CH_3$	Bayramoglu *et al*., 2013
1353	1314	1331.6	Vibration of the phosphate group Vibration of -C-O- C-N bend in aliphatic amines	Dos Santos Lima *et al*., 2011 Li et al., 2011 Saritha *et al*., 2014
1269	1240.5	1263.8	Vibration of COOH	Dos Santos *et al*., 2011
1229	ND	ND	Vibration of COOH	Saygideger *et al*. 2005
1168	1152.9	1151.4	Asymmetric tension of the -C-O-C- bridge of polysaccharides	Jiménez *et al*., 2011
1102.9 1015.6	ND 1024.8	ND 1013.6	C-O-H and -C-O- bend in polysaccharides	Bayramoglu *et al*., 2013 Dos Santos Lima *et al*., 2011 Jiménez *et al*., 2011

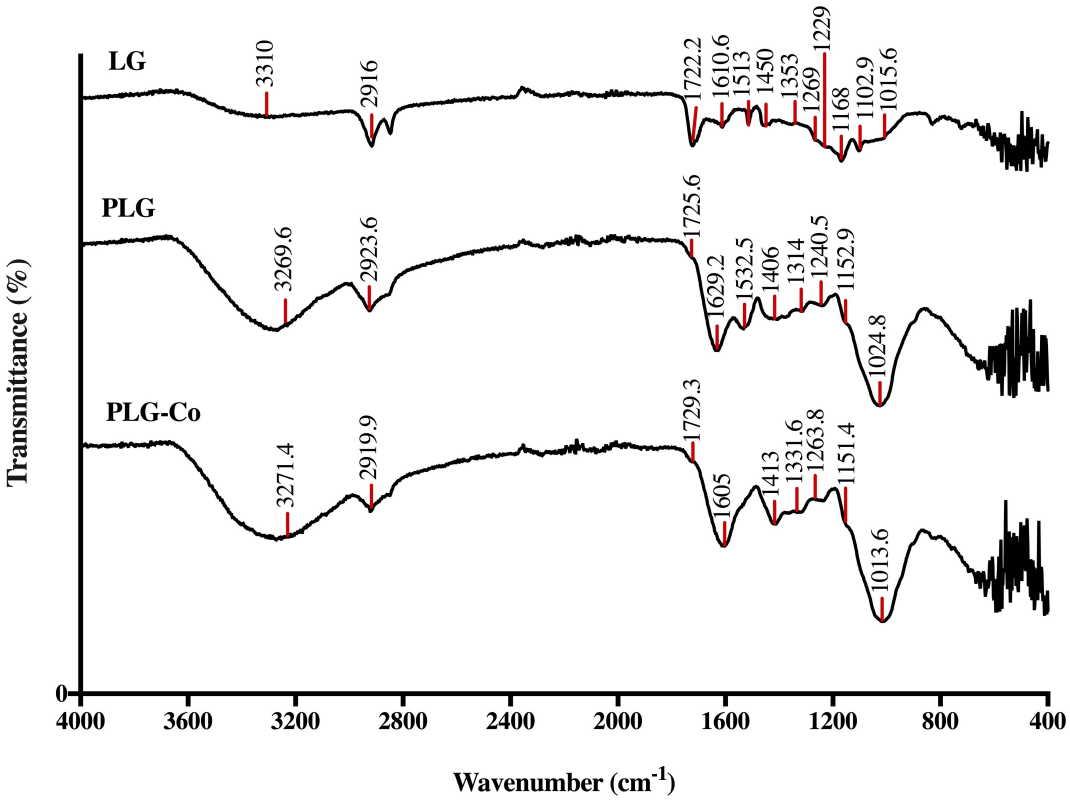

Fig. 8. FTIR of untreated *Lemna gibba* (LG) and the same plant material pretreated with K_2HPO_4 at 0.3 M (PLG) and saturated with Co^{2+} (PLG-Co).

This idea was confirmed by the displacement of the bands from 1450 cm^{-1} to 1406 cm^{-1} and from 1269 cm^{-1} to 1240 cm^{-1}, and the complete disappearance of the frequency at 1229 cm^{-1}. Furthermore, due to the relative increase in fiber (e.g., cellulose) stemming from the reduced amount of ash (according to proximate chemical analysis), a more definite band was found at 1024 cm^{-1}, typical of the -C-O- groups of polysaccharides. The data provided by the FTIR spectra are consistent with the previous discussion of the experimental findings as well as the proximate chemical analysis.

The pretreatment eliminated salts (making the active sites of cobalt biosorption more accessible) and increased the net negative charge of the biosorbent surface. Both changes favored interaction between the Co^{2+} ions and the functional groups responsible for the biosorption of the metal by PLG, resulting in a greater biosorption capacity. This phenomenon has been described in other reports on cobalt biosorption by materials pretreated with NaOH (Singh and Shukla, 2015).

With the aim of elucidating the possible functional groups responsible for the biosorption of Co^{2+}, the FTIR spectra of LG and PLG-Co were compared (Fig. 8). Based on the spectra, two groups play a role in the biosorption of Co^{2+} by pretreated *Lemna gibba*: the displacement of the frequency of the amide group from 1629.2 cm^{-1} to 1605 cm^{-1} and the disappearance of the vibration of the C-N and N-H (1532.5 cm^{-1}) bonds, characteristic of a peptide bond. Additionally, displacements were observed in the frequencies typical of carboxylic groups (1725 cm^{-1} to 1729 cm^{-1}, 1406 cm^{-1} to 1413 cm^{-1} and 1240 cm^{-1} to 1263.8 cm^{-1}) and the-C-O-H vibrations of the polysaccharides (1024 cm^{-1} to 1013 cm^{-1}) such as cellulose (Hernández-Botello *et al*., 2019). Hence, the amide and amine groups of the proteins and the carboxyl and hydroxyl groups of the carbohydrates are apparently the main functional groups involved in the biosorption of Co^{2+} by *Lemna gibba*. Similar results have been published for the removal of Co^{2+} by different materials (Vilvanathan and Shanthakumar, 2015; Anirudhan *et al*., 2016; Vilvanathan and Shanthakumar, 2016; Pipíska *et al*., 2017). Various authors have reported the importance

of the hydroxyl, amide, carboxyl and amine groups for the removal of diverse metals by the genus *Lemna*, including Hg^{2+}, Cr^{3+}, Cr^{6+}, Cu^{2+} (Rakhshaee *et al*., 2009), Pb^{2+} (Tang *et al*., 2013), and Au^{3+} (Saritha *et al*., 2014).

Conclusions

Lemna gibba presently proved to be a plant with great potential as a biosorbent for the detoxification of waters contaminated with Co^{2+}. The capacity of this plant to remove Co^{2+} from an aqueous solution was enhanced by the use of alkaline pretreatments, especially with KH_2PO_4 at 0.3 M. Furthermore, the pseudo-second order model was found to be the one that best fit the experimental data on the kinetics of biosorption of Co^{2+} by *Lemna gibba*. According to the comparison of the chemical characterization of untreated and the pretreated *Lemna gibba* (LG vs PLG), the pretreatment removed salts but not proteins from the plant material, which boosted the concentration of carbohydrates and thus led to a better availability of active sites. In addition, the KH_2PO_4-induced increase in electronegativity of the surface of the biosorbent at the pH assayed (7.0) favored the approach of Co^{2+} to the sorption sites. These changes probably explain the 109.3% greater biosorption capacity of PLG vs LG at equilibrium. The ATR-FTIR analysis shows that the hydroxyl, carboxyl, amide and amine groups of the carbohydrates and proteins present in the plant are responsible for the uptake of Co^{2+}.

Acknowledgements

The authors greatly appreciate the technical support provided by the Centro de Nanociencias y Micro y Nanotecnologías, IPN. This work was supported by the Secretaría de Investigación y Posgrado, IPN. The CONACyT awarded a graduate scholarship to three of the coauthors (J.L.R.-L., A.E.R.-R. and C.B.B.-C.). L.M.-B. and E.C.-U. hold grants from EDI-IPN, COFAA-IPN and SNI-CONACYT. The authors thank Bruce Allan Larsen for proofreading the manuscript.

Nomenclature

A	Initial velocity of adsorption (mg g^{-1} h-1)
$AICc$	Corrected Akaike information criterion
B	Constant related to the coverage of the surface and the activation energy for chemisorption (mg g^{-1})
BI	Behavior index (%)
C_{eq}	Residual concentration of Co^{2+} in the solution (mg L^{-1}) at equilibrium
C_i	Initial concentration of Co^{2+} in the solution (mg L^{-1}) at time to = 0 h
C_t	Residual concentration of Co^{2+} in the solution (mg L^{-1}) at time t
DMG	Dimethylglyoxime
k_1	Constant of the velocity of biosorption of the pseudo-first order model (min^{-1})
k_2	Constant of velocity of biosorption of the pseudo-second order model (g $mg^{-1}min^{-1}$)
k_p	Constant of the fractional power model (mg g^{-1} h^{-v})
LG	Biosorbent: untreated *Lemna gibba*
PLG	Biosorbent: the best of the pretreatments of *Lemna gibba* herein tested, selected for further experimentation
PLG-Co	Biosorbent: pretreated *Lemna gibba* that was saturated with Co^{2+}
q_{e-exp}	Experimental biosorption capacity at equilibrium (mg g^{-1})
q_{eq}	Biosorption capacity at equilibrium, as defined by the corresponding model (mg g^{-1})
q_t	Biosorption capacity at time t (mg g^{-1})
R^2	Correlation coefficient squared
SS	Sum of squares
Syx	Standard deviation of the residuals
t	Time (h)
t_{eq}	Time required to reach equilibrium (h)
t_f	Total time of the assay (h)
t_i	Initial time (0 h)
X	Concentration of the biosorbent employed (g L^{-1})

Greek symbols

v	Constant of velocity (h^{-1})
ζ	Zeta potential (mV)
ζ_0	Point of zero charge, zeta potential of 0, or isoelectric point of 0

References

Abbas, M., Kaddour, S. and Trari, M. (2014). Kinetic and equilibrium studies of cobalt adsorption on apricot stone activated carbón. *Journal of Industrial and Engineering Chemistry 20*, 745-751. https://doi.org/10.1016/j.jiec.2013.06.030

Abd El Hameed, A.H., Eweda, W.E., Abou-Taleb, K.A.A. and Mira, H.I. (2015). Biosorption of uranium and heavy metals using some local fungi isolated from phosphatic fertilizers. *Annals of Agricultural Sciences 60*, 345-351. https://doi.org/10.1016/j.aoas.2015.10.003

Abdelwahab, O., Fouad, Y.O., Amin, N.K. and Mandorb, H. (2015). Kinetic and thermodynamic aspects of cadmium adsorption onto raw and activated guava (*Psidium guajava*) leaves. *Environmental Progress & Sustainable Energy 34*, 351-358. https://doi.org/10.1002/ep.11991

Abdolali, A., Ngo, H.H., Guo, W., Zhou, J.L., Du, B., Wei, Q., Wang, X.C. and Nguyen, P.D. (2015). Characterization of a multi-metal binding biosorbent: Chemical modification and desorption studies. *Bioresource Technology 193*, 477-48. https://doi.org/10.1016/j.biortech.2015.06.123

Adeniyi, A.G. and Ighalo, J.O. (2019). Biosorption of pollutants by plant leaves: An empirical review. *Journal of Environmental Chemical Engineering 7*, 103100. https://doi.org/10.1016/j.jece.2019.103100

Ahluwalia, S.S. and Goyal, D. (2007). Microbial and plant derived biomass for removal of heavy metals from wastewater. *Bioresource Technology 98*, 2243-2257. https://doi.org/10.1016/j.biortech.2005.12.006

Anirudhan, T.S., Deepa, J.R. and Christa, J. (2016). Nanocellulose/nanobentonite composite anchored with multi-carboxyl functional groups as an adsorbent for the effective removal of Cobalt(II) from nuclear industry wastewater samples. *Journal of Colloid and Interface Science 467*, 307-320. https://doi.org/10.1016/j.jcis.2016.01.023

Argun, M.E., Dursun, S. and Karatas, M. (2009). Removal of Cd(II), Pb(II), Cu(II) and Ni(II) from water using modified pine bark. *Desalination 249*, 519-527. https://doi.org/10.1016/j.desal.2009.01.020

Azer, S.A. (2013). Taxonomic revision of genus *Lemna* L. (*Lemnaceae Gray*) in Egypt. *Annals of Agricultural Sciences 58*, 257-263. https://doi.org/10.1016/j.aoas.2013.07.015

Basha, S. and Murthy, Z.V.P. (2007). Kinetic and equilibrium models for biosorption of Cr(VI) on chemically modified seaweed, *Cystoseira indica. Process Biochemistry 42*, 1521-1529. https://doi.org/10.1016/j.procbio.2007.08.004

Bayramoglu, G., Adiguzel, N., Ersoy, G., Yilmaz, M. and Arica, M.Y. (2013). Removal of textile dyes from aqueous solution using amine-modified plant biomass of *A. caricum*: Equilibrium and kinetic studies. *Water, Air, & Soil Pollution 224*,1640-1656. https://doi.org/10.1007/s11270-013-1640-z

Bruce, B. and Weiner, D. (2011). Zeta Potential Analyzer. Brookhaven Instruments Corporation. Retrieved from http://www.brookhaveninstruments.com/theory

Bulgariu, D. and Bulgariu, L. (2016). Potential use of alkaline treated algae waste biomass as sustainable biosorbent for clean recovery of cadmium(II) from aqueous media: batch and column studies. *Journal of Cleaner Production 112*, 4525-4533. https://doi.org/10.1016/j.jclepro.2015.05.124

Cheang, C.Y. and Mohamed, N. (2016). Removal of cobalt from ammonium chloride solutions using a batch cell through an electrogenerative process. *Separation and Purification Technology 162*, 154-161. https://doi.org/10.1016/j.seppur.2016.02.023

Dabbagh, R., Ashtiani Moghaddam, Z. and Ghafourian, H. (2016). Removal of cobalt(II) ion from water by adsorption using intact and modified Ficus carica leaves as low-cost natural sorbent. *Desalination and Water Treatment 57*, 42, 19890-19902. https://doi.org/10.1080/19443994.2015.1103311

Daughton, C.G. (2014). Eco-directed sustainable prescribing: feasibility for reducing water contamination by drugs. *Science of the Total Environment 493*, 392-404. https://doi.org/10.1016/j.scitotenv.2014.06.013

Dos Santos Lima, L.K., Kleinübing, S.J., Da Silva, E.A. and Da Silva, M.G.C. (2011). Removal of chromium from wastewater using macrophyte *Lemna minor* as biosorbent. *Chemical Engineering Transactions 25*, 303-308. https://doi.org/10.3303/CET1125051

El-Sayed, M. and Nada, A.A. (2017). Polyethylenimine -functionalized amorphous carbon fabricated fromoil palm leaves as a novel adsorbent for Cr(VI) and Pb(II) from aqueous solution. *Journal of Water Process Engineering 16*, 296-308. http://dx.doi.org/10.1016/j.jwpe.2017.02.012

Fawzy, M.A., Hifney, A.F., Adam, M.S. and Al-Badaani, A.A. (2020). Biosorption of cobalt and its effect on growth and metabolites of *Synechocystis pevalekii* and *Scenedesmus bernardii*: Isothermal analysis. *Environmental Technology & Innovation 19*, 100953. https://doi.org/10.1016/j.eti.2020.100953

García-González, R., Gómez-Espinosa, R.M., Ávila-Pérez, P., Garcia-Gaitán, B., García-Rivas, J.L. and Zavala-Arce, R.E. (2016). Estudio de biosorción de Cu2+ en el criogel quitosano-celulosa. *Revista Mexicana de Ingeniería Química 15*, 311-322.

Giri, A.K. and Patel, R.K. (2012). Phytoaccumulation potential and toxicity of arsenic ions by *Eichhornia crassipes* in hydroponic system. *Journal of Bioremediation & Biodegradation 3*, 137-142. http://dx.doi.org/10.4172/2155-6199.1000137

Gramlich, A., Moradi, A.B., Robinson, B.H., Kaestner, A. and Schulin, R. (2011). Dimethylglyoxime (DMG) staining for semi-quantitative mapping of Ni in plant tissue. *Environmental and Experimental Botany 71*, 232-240. https://doi.org/10.1016/j.envexpbot.2010.12.008

Guerrero-Coronilla, I., Morales-Barrera, L. and Cristiani-Urbina, E. (2015). Kinetic, isotherm and thermodynamic studies of amaranth dye biosorption from aqueous solution onto water hyacinth leaves. *Journal of Environmental Management 152*, 99-108. https://doi.org/10.1016/j.jenvman.2015.01.026

Gupta, S., Sharma, S.K. and Kumar, A. (2019). Biosorption of Ni(II) ions from aqueous solution using modified *Aloe barbadensis* Miller leaf powder. *Water Science and Engineering 12*, 27-36. https://doi.org/10.1016/j.wse.2019.04.003

He, M., Zhu, Y., Yang, Y., Han, B. and Zhang, Y. (2011). Adsorption of cobalt(II) ions from aqueous solutions by palygorskite. *Applied Clay Science 54*, 292-296. https://doi.org/10.1016/j.clay.2011.09.013

Hernandez-Botello, M., Barriada-Pereira, J., Sastre de Vicente, M., Mendoza-Pérez, J., Chanona-Pérez, J., López-Cortez, M., and Téllez-Medina, D. (2019). Determination of biosorption mechanism in biomass of agave, using spectroscopic and microscopic techniques for the purification of contaminated water. *Revista Mexicana De Ingeniería Química 19*, 215-226. https://doi.org/10.24275/rmiq/IA501

Hernández-Estévez, A. and Cristiani-Urbina, E. (2014). Nickel(II) biosorption from aqueous solutions by shrimp head biomass. *Environmental Monitoring and Assessment 186*, 7987-7998. https://doi.org/10.1007/s10661-014-3981-5

Horwitz, W. and Latimer, G.W. Jr. (2005). *Oficial Methods of Analysis of AOAC International*, 18th ed. AOAC International: Gaithersburg, MD, USA.

Huang, W., Wang, S., Zhu, Z., Li, L., Yao, X., Rudolph, V. and Haghseresht, F. (2008). Phosphate removal from wastewater using red mud. *Journal of Hazardous Materials 158,* 35-42. https://doi.org/10.1016/j.jhazmat.2008.01.061

Huang, Y., Li, S., Lin, H. and Chen, J. (2014). Fabrication and characterization of mesoporous activated carbon from *Lemna minor* using one-step H_3PO_4 activation for Pb(II) removal. *Applied Surface Science 317*, 422-431. https://doi.org/10.1016/j.apsusc.2014.08.152

Ighalo, J.O. and Adeniyi, A.G. (2020). A mini-review of the morphological properties of biosorbents derived from plant leaves. *SN Applied Sciences 2*, 509. https://doi.org/10.1007/s42452-020-2335-x

Jacques, R.A., Bernardi, R., Caovila, M., Lima, E.C., Pavan, F.A., Vaghetti, J.C.P. and Airoldi, C. (2007). Removal of Cu(II), Fe(III), and Cr(III) from aqueous solution by aniline grafted silica gel. *Separation Science and Technology 42*, 591-609. https://doi.org/10.1080/01496390601069952

Javaid, A., Bajwa, R. and Manzoor, T. (2011). Biosorption of heavy metals by pretreated biomass of *Aspergillus niger*. *Pakistan Journal of Botany 43*, 419-425.

Jiménez, G., Rodriguez, E., Contreras, M., Valbuena, A. and Colina, M. (2011). Obtención de carboximetil celulosa usando *Lemna* como materia prima. *Revista Iberoamericana de Polímeros 12*, 334-341.

Khajavian, M., Wood, D.A., Hallajsani, A. and Majidian, N. (2019). Simultaneous biosorption of nickel and cadmium by the brown algae *Cystoseria indica* characterized by isotherm and kinetic models. *Applied Biological Chemistry 62*, 69. https://doi.org/10.1186/s13765-019-0477-6

Khataee, A.R., Movafeghi, A., Torbati, S., Salehi Lisar, S.Y. and Zarei, M. (2012). Phytoremediation potential of duckweed (*Lemna minor* L.) in degradation of C.I. Acid Blue 92: Artificial neural network modeling. *Ecotoxicology and Environmental Safety 80*, 291-298. https://doi.org/10.1016/j.ecoenv.2012.03.021

Khokhar, A., Siddique, Z. and Misbah. (2019). Removal of heavy metal ions by chemically treated *Melia azedarach* L. leaves. *Journal of Environmental Chemical Engineering 3*, 944-952. https://doi.org/10.1016/j.jece.2015.03.009

Khosravihaftkhany, S., Morad, N., Abdullah, A.Z., Tenga, T.T. and Ismail, N. (2015). Biosorption of Pb(II) and Fe(III) from aqueous cosolutions using chemically pretreated oil palm fronds. *RSC Advances 5*, 106498. https://doi.org/10.1039/C5RA15325E

Landolt, E. and Kandeler, R. (1987). *The Family of Lemnaceae - A Monographic Study,* vol 2 - *Biosystematic Investigations in the Family of Duckweeds* (Lemnaceae), vol 4. Veröffentlichungen des Geobotanischen Institutes ETH, Stiftung Rubel, Zürich.

Leyssens, L., Vinck, B., Van Der Straeten, C., Wuyts, F. and Maes, L. (2017). Cobalt toxicity in humans- A review of the potential sources and systemic health effects. *Toxicology 387*, 43-56. http://dx.doi.org/10.1016/j.tox.2017.05.015

Li, S., Zheng F., Yang, H. and Ni J. (2011). Thorough removal of inorganic and organic mercury from aqueous solutions by adsorption on *Lemna minor* powder. *Journal of Hazardous Materials 186*, 423-429. https://doi.org/10.1016/j.jhazmat.2010.11.009

Mamba, B.B., Dlamini, N.P. and Mulaba-Bafubiandi, A.F. (2009). Biosorptive removal of copper and cobalt from aqueous solutions: *Shewanella* spp. put to the test. *Physics and Chemistry of the Earth, Parts A/B/C 34,* 841-849. https://doi.org/10.1016/j.pce.2009.07.009

Martín-Lara, M.A., Blázquez, G., Ronda, A., Pérez, A. and Calero, M. (2013). Development and characterization of biosorbents to remove heavy metals from aqueous solutions by chemical treatment of olive stone. *Industrial & Engineering Chemistry Research 52*, 10809-10819. https://doi.org/10.1021/ie401246c

Martínez-Guerra, E., Gude, V.G., Mondala, A., Holmes, W. and Hernandez, R. (2014). Extractive-transesterification of algal lipids under microwave irradiation with hexane as solvent. *Bioresource Technology 156*, 240-247. https://doi.org/10.1016/j.biortech.2014.01.026

Moradi, P., Hayati, S. and Ghahrizadeh, T. (2020). Modeling and optimization of lead and cobalt biosorption from water with Rafsanjan pistachio shell, using experiment based models of ANN and GP, and the grey wolf optimizer. *Chemometrics and Intelligent Laboratory Systems 202*, 104041. https://doi.org/10.1016/j.chemolab.2020.104041

Moreno-Rivas, S.C., Armenta-Corral, R.I., Frasquillo-Félix, M.C., Lagarda-Díaz, I., Vázquez-Moreno, L. and Ramos-Clamont Montfort, G. (2016). Biosorption of cadmium from aqueous solution by baker's yeast (*Saccharomyces cerevisiae*). *Revista Mexicana de Ingeniería Química 15*, 843-857. Retrieved from http://rmiq.org/ojs311/index.php/rmiq/article/view/1049

Myśliwiec, D., Chyliska, M., Szymanska-Chargot, M., Chibowski, S. and Zdunek, A. (2016). Revision of adsorption models of xyloglucan on microcrystalline cellulose. *Cellulose 23*, 2819-2829. https://doi.org/10.1007/s10570-016-0995-x

Nadeem, R., Nadeem Zafar, M., Afzal, A., Asif Hanif, M. and Saeed, R. (2014). Potential of NaOH pretreated *Mangifera indica* waste biomass for the mitigation of Ni(II) and Co(II) from aqueous solutions. *Journal of the Taiwan Institute of Chemical Engineers 45*, 967-972. http://dx.doi.org/10.1016/j.jtice.2013.09.012

Patel, H. and Vashi, R.T. (2013). A comparison study of removal of methylene blue dye by adsorption on neem leaf powder (NLP) and activated NLP. *Journal of Environmental Engineering and Landscape Management 21*, 36-41. https://doi.org/10.3846/16486897.2012.671772

Pei, Y., Xu, G., Wu, X., Tang, K. and Wang, G. (2019). Removing Pb(II) ions from aqueous solution by a promising absorbent of tannin-immobilized cellulose microspheres. *Polymers 11*, 548. https://doi.org/10.3390/polym11030548

Pipíška, M., Richveisová, B.M., Frišták, V., Horník, M., Remenárová, L., Stiller, R. and Soja, G. (2017). Sorption separation of cobalt and cadmium by straw-derived biochar: a radiometric study. *Journal of Radioanalytical and Nuclear Chemistry 311*, 85-97. https://doi.org/10.1007/s10967-016-5043-7

Rakhshaee, R., Giahi, M. and Pourahmad, A. (2009). Studying effect of cell wall's carboxyl-carboxylate ratio change of *Lemna minor* to remove heavy metals from aqueous solution. *Journal of Harzardous Materials 163*, 165-173. https://doi.org/10.1016/j.jhazmat.2008.06.074

Ramírez-Rodríguez, A., Reyes-Ledezma, J., Chávez-Camarillo, G., Cristiani-Urbina, E., and Morales-Barrera, L. (2018). Cyclic biosorption and desorption of acid red 27 onto *Eichhornia crassipes* leaves. *Revista Mexicana De Ingeniería Química 17*, 1121-1134. Retrieved from https://doi.org/10.24275/uam/izt/dcbi/revmexingquim/2018v17n3/Ramirez

Reyes-Ledezma, J.L. (2017) *Biosorción de Co(II) a partir de soluciones acuosas por Lemna sp. Tesis de maestría en Ciencias Quimicobiológicas*, Instituto Politécnico Nacional, Ciudad de México, México.

Reyes-Ledezma, J.L., Uribe-Ramírez, D., Cristiani-Urbina, E. and Morales-Barrera, L. (2020). Biosorptive removal of acid orange 74 dye by HCl-pretreated Lemna sp. *PLoS ONE 15*, e0228595. https://doi.org/10.1371/journal.pone.0228595

Salazar-Rabago, J.J. and Leyva-Ramos, R. (2016). Novel biosorbent with high adsorption capacity prepared by chemical modification of white pine (*Pinus durangensis*) sawdust. Adsorption of Pb(II) from aqueous solutions. *Journal of Environmental Management 169*, 303-312. https://doi.org/10.1016/j.jenvman.2015.12.040

Saritha, K., Saraswathi, U., Singaravelu, G., Revathi, S. and Jayanthi, V. (2014). Biological synthesis and characterization of gold nanoparticles using *Lemna minor. Asian Journal of Pharmaceutical and Clinical Research 7*,165-167.

Saygideger, S., Gulnaz, O., Istifli, E.S. and Yucel, N. (2005). Adsorption of Cd(II), Cu(II) and Ni(II) ions by *Lemna minor* L.: Effect of physicochemical environment. *Journal of Hazardous Materials 126*, 96-104. https://doi.org/10.1016/j.jhazmat.2005.06.012

Schneider, I.A.H., Rubio, J. and Smith, R.W. (2001). Biosorption of metals onto plant biomass: Exchange adsorption or surface precipitation. *International Journal of Mineral Processing 62*, 111-120. https://doi.org/10.1016/S0301-7516(00)00047-8

Shahat, A., Awual, M.R. and Naushad, M. (2015). Functional ligand anchored nanomaterial based facial adsorbent for cobalt(II) detection and removal from water samples. *Chemical Engineering Journal 271*, 155-163. https://doi.org/10.1016/j.cej.2015.02.097

Singh, S.A. and Shukla, S.R. (2015). Adsorptive removal of cobalt ions on raw and alkali-treated lemon peels. *International Journal of Environmental Science and Technology 13*, 165-178. https://doi.org/10.1007/s13762-015-0801-6

Suazo-Madrid, A., Morales-Barrera, L., Aranda-García, E. and Cristiani-Urbina, E. (2011). Nickel(II) biosorption by *Rhodotorula glutinis*. *Journal of Industrial Microbiology & Biotechnology 38*, 51-64. https://doi.org/10.1007/s10295-010-0828-0

Tang, Y., Chen, L., Wei, X., Yao, Q. and Li, T. (2013). Removal of lead ions from aqueous solution by the dried aquatic plant, *Lemna perpusilla* Torr. *Journal of Hazardous Materials 244-245*, 603-612. https://doi.org/10.1016/j.jhazmat.2012.10.047

Tejada-Tovar, C., Bonilla Mancilla, H., Del Pino Moreyra, J., Villabona-Ortiz, A., and Ortega-Toro, R. (2020). Effect of the adsorbent dose in Pb(II) removal by using sugar cane bagasse: Kinetics and isotherms. *Revista Mexicana de Ingeniería Química 19*, 1413-1423. https://doi.org/10.24275/rmiq/IA1101

Teymouri, P., Ahmadi, M., Akbar Babaei, A., Ahmadi, K. and Jaafarzadeh, N. (2013). Biosorption studies on NaCl-modified Ceratophyllum demersum: removal of toxic chromium from aqueous solution. *Chemical Engineering Communications 200*, 1394-1413. http://dx.doi.org/10.1080/00986445.2012.744748

Villabona-Ortíz, A., Tejada-Tovar, C., and Ortega-Toro, R. (2019). Modelling of the adsorption kinetics of chromium (VI) using waste biomaterials. *Revista Mexicana de Ingeniería Química 19*, 401-408. https://doi.org/10.24275/rmiq/IA650

Vilvanathan, S. and Shanthakumar, S. (2015). Biosorption of Co(II) ions from aqueous solution using *Chrysanthemum indicum*: Kinetics, equilibrium and thermodynamics. *Process Safety and Environmental Protection 96*, 98-110. https://doi.org/10.1016/j.psep.2015.05.001

Vilvanathan, S. and Shanthakumar, S. (2016) Removal of Ni(II) and Co(II) ions from aqueous solution using teak (*Tectona grandis*) leaves powder: adsorption kinetics, equilibrium and thermodynamics study. *Desalination and Water Treatment 57*, 3995-4007. https://doi.org/10.1080/19443994.2014.989913

Volesky, B. (2003). Biosorption process simulation tools. *Hydrometallurgy 71*, 179-190. https://doi.org/10.1016/S0304-386X(03)00155-5

Vullo, D.L., Ceretti, H.M., Daniel, M.A., Ramírez, S.A.M. and Zalts, A. (2008). Cadmium, zinc and copper biosorption mediated by *Pseudomonas veronii 2E*. *Bioresource Technology 99*, 5574-5581. https://doi.org/10.1016/j.biortech.2007.10.060

Wang, J. and Chen, C. (2006). Biosorption of heavy metal by *Saccharomyces cerevisiae*: A review. *Biotechnology Advances 24*, 427-451. https://doi.org/10.1016/j.biotechadv.2006.03.001

Yazici, H., Kiliç¸ M. and Solak, M. (2008). Biosorption of copper(II) by *Marrubium globosum* subsp. globosum leaves powder: Effect of chemical pretreatment. *Journal of Hazardous Materials 151*, 669-675. https://doi.org/10.1016/j.jhazmat.2007.06.042

Zafar, M.N., Saeed, M., Nadeem, R., Sumrra, S.H., Shafqat, S.S. and Qayyum, M.A. (2019). Chemical pretreatments of *Trapa bispinosa*'s peel (TBP) biosorbent to enhance adsorption capacity for Pb(II). *Open Chemistry 17*, 325-336. https://doi.org/10.1515/chem-2019-0031

Zetina, C.P., Reta, M.J.L., Orteaga, C.M.E., Orteaga, J.E., Sánchez-Torres, M.T.E., Herrera, H.J.G. and Becerril, H.M. (2010). Utilización de la lenteja de agua (*Lemnaceae*) en la producción de tilapia (*Oreochromis* spp.). *Archivos de Zootecnia 59*,133-155. https://doi.org/10.21071/az.v59i232.4911

Zhao, X., Moates, G.K., Wellner, N., Collins, S.R.A., Coleman, M.J. and Waldron, K.W. (2014). Chemical characterisation and analysis of the cell wall polysaccharides of duckweed (*Lemna minor*). *Carbohydrate Polymers 111*, 410-418. https://doi.org/10.1016/j.carbpol.2014.04.079